FEBS Letters 581 (2007) 1403–1408

The role of Asp-295 in the catalytic mechanism of *Leuconostoc mesenteroides* sucrose phosphorylase probed with site-directed mutagenesis

Mario Mueller, Bernd Nidetzky*

Institute of Biotechnology and Biochemical Engineering, Graz University of Technology, Petersgasse 12, A-8010 Graz, Austria

Received 11 January 2007; revised 26 February 2007; accepted 26 February 2007

Available online 5 March 2007

Edited by Hans Eklund

Abstract **Replacements of Asp-295 by Asn (D295N) and Glu (D295E) decreased the catalytic center activity of *Leuconostoc mesenteroides* sucrose phosphorylase to about 0.01% of the wild-type level (k_{cat} = 200 s^{-1}). Glucosylation and deglucosylation steps of D295N were affected uniformly, ~$10^{4.3}$-fold, and independently of leaving group ability and nucleophilic reactivity of the substrate, respectively. pH dependences of the catalytic steps were similar for D295N and wild-type. The 10^5-fold preference of the wild-type for glucosyl transfer compared with mannosyl transfer from phosphate to fructose was lost in D295N and D295E. Selective disruption of catalysis to *glucosyl* but not *mannosyl* transfer in the two mutants suggests that the side chain of Asp-295, through a strong hydrogen bond with the equatorial sugar 2-hydroxyl, stabilizes the transition states flanking the β-glucosyl enzyme intermediate by ⩾ 23 kJ/mol.**

Keywords: Sucrose phosphorylase; Glycoside hydrolase; Family GH-13; Transition state; 2-Hydroxyl; Hydrogen bonding

1. Introduction

Leuconostoc mesenteroides sucrose phosphorylase (*Lm*SPase) catalyzes the reversible conversion of sucrose (α-D-glucopyranosyl 2-β-D-fructofuranoside) and phosphate into α-D-glucose 1-phosphate (αG1P) and D-fructose. Glucosyl transfer to and from phosphate is promoted by Asp-196 and Glu-237 whose side chains function in catalysis as nucleophile [1] and acid–base [2] respectively. Fig. 1A depicts the proposed two-step mechanism of the phosphorylase. Based on sequence similarity, *Lm*SPase has been classified into glycoside hydrolase family GH-13 [4], a large and functionally diverse group of enzymes that include amylase and α-glucanotransferase as their most prominent activities [4,5]. Results from sequence alignments, X-ray structures, and site-directed mutagenesis studies have delineated a common active-site pattern for enzymes of family GH-13, in which Asp-196, Glu-237, and Asp-295 of *Lm*SPase (or their positional homologs) constitute a conserved triad of catalytic residues [5–10]. Although Asp-295 is often referred to as a "transition state stabilizer" in the literature, a unified description at the molecular level of how it affects catalysis in glycoside hydrolases of family GH-13 is not available. One plausible mechanism for Asp-295 is that hydrogen bonding interactions of the carboxylate side chain with hydroxyls at carbons 2 and 3 of the glucosyl residue bound at subsite −1 have a role in substrate distortion and become optimized in the transition states flanking the covalent β-glucosyl enzyme intermediate [11–13] (Fig. 1B). An additional or perhaps alternative role of Asp-295 is activation of Glu-237 for function as the catalytic proton donor [5,8,13–16] (Fig. 1C). Here, we report on results of experiments designed to distinguish between the different mechanistic proposals for Asp-295 and portray the role of the conserved Asp residue in each step of catalysis by *Lm*SPase (see Fig. 1).

2. Materials and methods

α-D-Mannose 1-phosphate (αM1P) was from Sigma–Aldrich. Reagents and chemicals for MS analysis were reported elsewhere [17]. All other materials were described in a recent paper [1].

2.1. Site-directed mutagenesis, enzyme production and purification

Mutations causing site-specific substitution of Asp-295 by Asn and Glu at the protein level were introduced with the two-stage PCR method, employing some modifications of the original protocol [1]. The following pairs of oligonucleotide primers were used where the mismatched codons are indicated in bold. D295N: 5′-GGACACGCATA**AT**GGTATTGGTG-3′ (forward primer), 5′-CACCAATACC**ATT**ATGCGTGTCC-3′ (reverse primer); D295E: 5′-GGACACGCAT**GAA**GGTATTGGTG-3′ (forward primer), 5′-CACCAATACC**TTC**-ATGCGTGTCC-3′ (reverse primer). Sequenced plasmid vectors harboring the mutagenized genes were transformed into *E. coli* JM109, and recipient strains were grown at 37 °C in Luria–Bertani medium containing 0.12 g/l ampicillin. Induction of gene expression and recombinant protein production were carried out exactly as reported elsewhere [1]. D295N and D295E were purified using the protocol employed previously for the isolation of the wild-type and a D196A mutant thereof [1]. Purification was monitored by SDS–PAGE.

2.2. Kinetic characterization

Initial rate measurements were carried out at 30 °C in 20 mM MES buffer, pH 7.0, using reported discontinuous assays for phosphorolysis and synthesis of sucrose as well as arsenolysis of αG1P [1]. Typical concentrations of D295N and D295E were 50–400 μg/ml, and incubation times of about 1–2 h were used. The concentrations of released αG1P

*Corresponding author. Fax: +43 316 873 8434.
E-mail address: bernd.nidetzky@tugraz.at (B. Nidetzky).

Abbreviations: αG1P, α-D-glucose 1-phosphate; αM1P, α-D-mannose 1-phosphate; SPase, sucrose phosphorylase; *Lm*SPase, SPase from *Leuconostoc mesenteroides*; *Ba*SPase, SPase from *Bifidobacterium adolescentis*

0014-5793/$32.00
doi:10.1016/j.febslet.2007.02.060

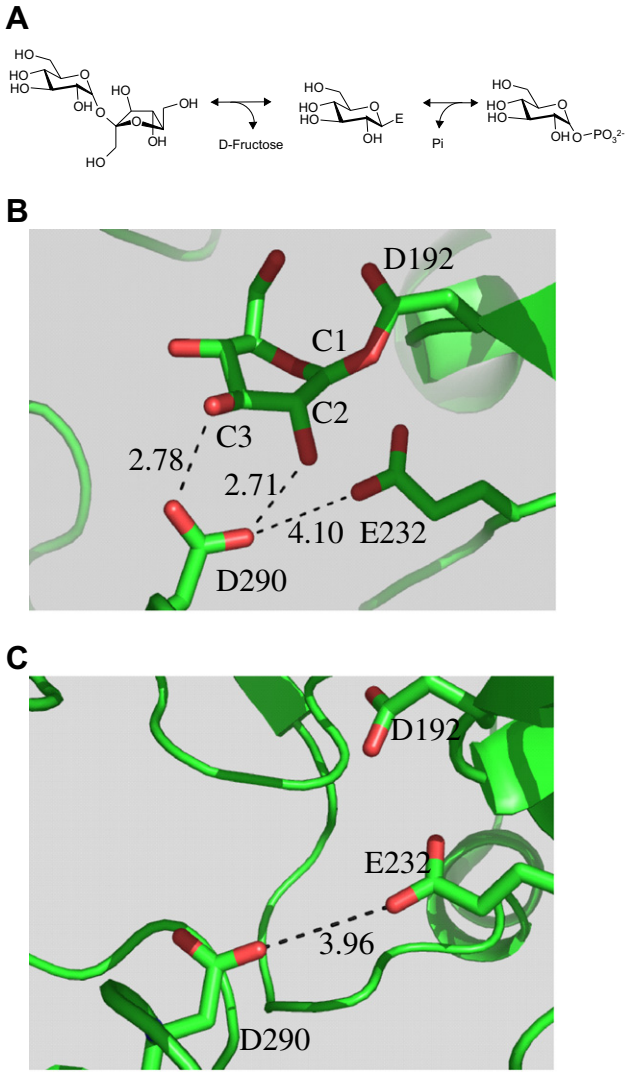

Fig. 1. (A) Proposed reaction mechanism of SPase, and (B and C) close-up structures of the catalytic subsite in the covalent glucosyl enzyme intermediate and the free enzyme, respectively. In the absence of one of the natural nucleophiles (phosphate or fructose) the covalent intermediate can be intercepted by water or other suitable nucleophiles [3]. Panels B and C are drawn using X-ray structures of *Ba*SPase [9,10]. H-bond distances are in Å.

(phosphorolysis), phosphate (synthesis), and glucose (arsenolysis) were determined using published analytical methods [1]. Glucose was measured using glucose oxidase and detection of the H_2O_2 produced with peroxidase and, in a modification of the original protocol [18], *o*-dianisidine instead of phenol and 4-aminophenazone. Nonenzymatic background rates were measured in suitable controls lacking phosphorylase or glucosyl donor substrate and if required, used for correction of the enzymatic rates. Kinetic parameters were obtained from initial rates recorded under conditions in which the concentration of the glucosyl donor was varied at a constant, wherever possible saturating, concentration of the glucosyl acceptor, or vice versa. The molar enzyme concentration, derived from protein concentration measurements using the Bio-Rad dye binding method with BSA as the standard, was the basis for the calculation of the reported catalytic center activities (k_{cat}). Note that a reliable method for titration of active sites is not available.

2.3. Specificity for glycosyl donor and acceptor substrates

αM1P was tested as an alternative glycosyl donor substrate of wild-type *Lm*SPase, D295N, and D295E. Reaction mixtures contained 5 mM αM1P and 200 mM fructose dissolved in 20 mM MES buffer, pH 7.0. The enzyme concentration was about 200 μg/ml, and incubations were carried out at 30 °C. The release of phosphate in time was measured. Reactions with αG1P were carried out under exactly identical conditions, except that a lower enzyme concentration of the wild-type (0.3 μg/ml) had to be used. Enzyme activities with αM1P and αG1P were compared at similar levels of conversion of glycosyl donor (⩽20%).

L-Arabitol was examined as an acceptor substrate for transglucosylation reactions catalyzed by wild-type enzyme and D295 mutants thereof. In the absence of acceptor, a significant portion of αG1P (5 mM) is hydrolyzed by each of the three enzymes. Under hydrolysis-only conditions, the rates of conversion of αG1P (V_{G1P}) and release of phosphate (V_{Pi}) will be matched with the rate of release of glucose (V_{Glc}). However, when the glucosyl enzyme intermediate partitions between reactions with an external acceptor and water, V_{Pi} will have a greater value than V_{Glc}. The rate ratio V_{Pi}/V_{Glc} is expected to exhibit a linear dependence on the concentration of acceptor (0–180 mM L-arabitol) with a slope K_{trans} that characterizes the relative transfer specificity of the enzyme. Reactions utilized 0.5 μg/ml wild-type and 250 μg/ml D295N and D295E. V_{Pi} and V_{Glc} were measured.

2.4. pH dependence studies

Initial rates of phosphorolysis and synthesis of sucrose were measured in the pH range 5.0–8.0 using 20 mM MES buffer. Solutions were prepared at the reaction temperature of 30 °C, and pH values were checked immediately before and after the assay. The presence of phosphate or αG1P in concentrations of 2 mM or greater ensured stable pH values below pH 5.2 and above pH 7.2 where MES (p*K* 6.2) does not provide buffering capacity. Control experiments in which NaCl concentrations of up to 100 mM was added to standard enzyme assays at pH 7.0 showed no effect of the salt, indicating that the change in ionic strength (from 1.2 mM at pH 5.0 to 20 mM at pH 8.0) resulting from buffer ionization in the pH range studied should not interfere with determination of the pH dependence of kinetic parameters.

pH profiles of $\log k_{cat}$ and $\log(k_{cat}/K_m)$ where K_m is the apparent Michaelis constant were fitted with the appropriate equation, where Eq. (1) describes a $\log Y$ versus pH curve that decreases with a slope of +1 below pK_1, and Eq. (2) describes a bell-shaped curve for $\log Y$ that decreases with slopes of +1 and −1 below pK_1 and above pK_2, respectively

$$\log Y = \log(C/(1 + [H^+]/K_1)) \quad (1)$$

$$\log Y = \log(C/(1 + [H^+]/K_1 + K_2/[H^+])) \quad (2)$$

where Y is k_{cat} or k_{cat}/K_m, C is the pH-independent value of Y at the optimal state of protonation, K_1 and K_2 are macroscopic dissociation constants, and $[H^+]$ is the proton concentration.

2.5. Other analytical procedures

2.5.1. Circular dichroism spectroscopy. Far-UV CD spectra of protein solutions (0.4 mg/ml; 20 mM MES buffer, pH 7.0) were recorded at 25 °C in the wavelength range 195–250 nm with a JASCO J-715 Spectropolarimeter using a Hellmar 0.1 mm path-length cylindrical cell and the following instrument settings: 0.2 nm step resolution; 50 nm/min scan speed; 1 sec response time; 1 nm bandwidth. Triplicate spectra were averaged and corrected with a buffer spectrum before converting the CD signal to mean residue ellipticity using the program Dichroweb [19].

2.5.2. Mass spectrometry. Protein structural characterization by MS was performed using a LCQ Deca XPplus ion trap mass spectrometer (Thermo) equipped with a nano-electrospray ionization (ESI) source coupled to a nanoLC system (LC-packings, Amsterdam, The Netherlands) consisting of FAMOS™ autosampler, SWITCHOS™ loading system, and ULTIMATE™ dual gradient system. For peptide mass fingerprinting, in-gel tryptic digestion of the protein sample was performed using a reported protocol [17]. Twenty microliters of peptide extract dissolved in 0.1% (per vol.) formic acid were trapped on a LC Packings C18 Pep-Map precolumn (5 μm, 100 Å, 300-μm inner diameter × 1 mm) with a total loading time of 5 min and a sample solution flow rate of 20 μl/min. The loaded mixture was then flushed to a nanoLC separation column of the same type (75-μm inner diameter × 150 mm) with a flow rate of 300 nl/min, and peptides were eluted using a 60-min linear gradient of 5–50% (per vol.) acetonitrile in 0.3% (per vol.) formic acid. The column effluent was directed to a NanoSpray tip (Pico-Tip™ Emitter), and positive ions formed by the electro-